A waveguide model of the return stroke channel with a "metamaterial" corona

Nikolai G. Lehtinen[1]

Received 6 April 2011; revised 19 October 2011; accepted 6 November 2011; published 12 January 2012.

[1] We model the lightning return stroke channel as a three layer cylindrical waveguide, consisting of (1) highly conducting thin core channel; (2) "metamaterial" corona, i.e., corona with an effective bulk anisotropic dielectric permittivity tensor which is due to the fine structure of leaders branching away from the main channel; and (3) the surrounding non-conducting air. The lowest axially symmetric TM mode in this waveguide represents the return stroke current wave. We find time- and space-domain solutions for the current wave in a channel connected to the ground driven by an axial current of Bruce-Golde model temporal shape concentrated at the point of the channel connection to the ground. The front of the current wave is found to be dispersed, and the speed of the front is significantly (by a factor of 5–10 for some parameters) slower than the speed of light. The calculated radial electric field is found to be consistent with experimental measurements. When the second layer of the waveguide is filled with an isotropic material, the slowdown of the wavefront is found to be smaller. The time- and space-domain calculations are also supported by the numerical solution of a dispersion equation, which shows that the phase velocity may be significantly less than the speed of light.

Citation: Lehtinen, N. G. (2012), A waveguide model of the return stroke channel with a "metamaterial" corona, *Radio Sci.*, *47*, RS1003, doi:10.1029/2011RS004749.

1. Introduction

[2] The return stroke is the most energetic process in a lightning flash, during which the highest currents occur and which therefore may be the most responsible for the lightning-related damage. An overview of the contemporary understanding of this process is given, for example, by *Rakov and Rachidi* [2009]. In this work, we introduce a new waveguide model of the return-stroke channel, which belongs to the class of electromagnetic models [*Baba and Rakov*, 2007], and discuss its connection with a distributed-circuit, or transmission-line (TL) model. Previous waveguide models of the return stroke channel include conducting cylindrical core [*Volland*, 1981], the cylindrical core with inclusion of the effects of the conducting Earth [*Baba and Rakov*, 2005], highly conducting thin core surrounded by a perfectly conducting cylindrical shell corona shield, which may be further developed a multifractal approach [*Wang*, 2010], and a wire immersed in an artificial isotropic dielectric medium [*Moini et al.*, 2000].

[3] We explore the possibility that the corona may be conducting differently in radial and axial directions, namely high radial and low axial conductivity. The motivation for this comes from two directions:

[4] 1. The recently developed fractal lightning model [*Liang et al.*, 2010; *Carlson et al.*, 2011] show the short leaders branching away from the main channel (B. Carlson and C. Liang, personal communication, 2011). These branches may increase radial conductivity of the corona, while there is no conductivity in axial direction, across the branches (see Figure 1a).

[5] 2. The high conductivity in radial direction allows charges to flow to the outer boundary of the corona, thereby increasing the capacitance C per unit length of the channel, while the low conductivity in the axial direction restricts the axial currents to flow only in the highly conducting core of the channel, thereby fixing the inductance L per unit length to be determined by the radius of the core. This charge/current distribution in the lightning channel was also proposed for an isotropic corona [*Rakov*, 1998], but is obviously facilitated by the anisotropicity. The phase velocity of the wave propagating along such a channel is $v_{ph} = 1/\sqrt{LC}$ (see more of this discussion in section 4.1), which thus becomes smaller than the speed of light, providing a possible explanation to observed speeds of return strokes of $c/3$–$c/2$ [*Rakov*, 2007].

[6] In this paper, we use the "physics" $\propto e^{-i\omega t}$ convention and work in cylindrical system of coordinates (ρ, ϕ, z), such that z-axis coincides with the axis of the cylindrically symmetric return stroke channel. We model the wave

[1]Department of Electrical Engineering, Stanford University, Stanford, California, USA.

0048-6604/12/2011RS004749

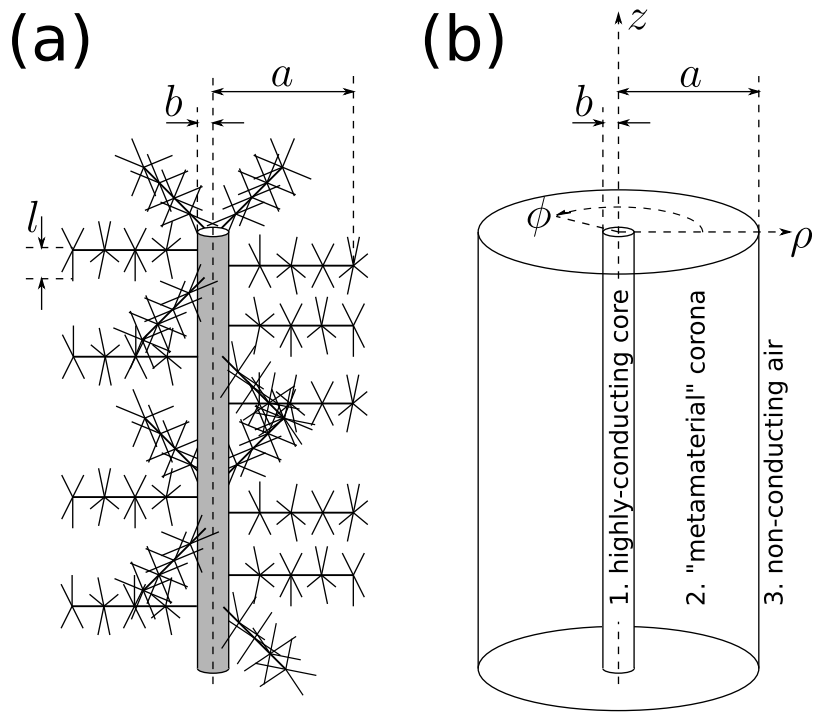

Figure 1. The return stroke channel: (a) the corona with complicated anisotropy and (b) the waveguide model including the "metamaterial" corona.

propagating along the channel as $\propto \exp(ik_z z)$. In many expressions we use the free-space wave number $k_0 = \omega/c$.

2. Waveguide Model

2.1. Corona "Metamaterial"

[7] We model the corona as a conducting bulk material. The effective (long-wave) conductivity is anisotropic since it is due to the branch leaders in the corona which have an anisotropic distribution. We assume it is highly conducting in the radial direction, due to branches extending from the core of the channel to the outer boundary of the corona, as shown in Figure 1a. We prefer to work with the dielectric permittivity tensor $\hat{\varepsilon}$ defined as

$$\hat{\varepsilon}(\omega) = \hat{K} + \frac{i\hat{\sigma}}{\varepsilon_0\omega} = \hat{K} + i\hat{N}$$

where $\hat{K} = \mathrm{Re}\hat{\varepsilon}$ is the real part due to polarization and $\hat{N} = \hat{\sigma}/(\varepsilon_0\omega) = \Im\hat{\varepsilon}$ is due to conductivity. In the most general (non-diagonal) case, $\hat{K}$ and $i\hat{N}$ are hermitian and anti-hermitian parts of $\hat{\varepsilon}$; however, here we only work with diagonal $\hat{\varepsilon}$. Both K and N are dimensionless. Thus, if we write tensor $\hat{\varepsilon}$ as

$$\hat{\varepsilon} = \begin{pmatrix} \varepsilon_\rho & 0 & 0 \\ 0 & \varepsilon_\phi & 0 \\ 0 & 0 & \varepsilon_z \end{pmatrix} \quad (1)$$

we have $\varepsilon_\rho = K_\rho + iN_\rho$, where $N_\rho \gg 1$ due to high conductivity of the branch leader channels, and we will take $K_\rho = 1$ (no contribution due to polarization). The dielectric permittivities in azimuthal (ε_ϕ) and axial (ε_z) directions will be assumed not to have a highly conducting contribution, but they may also be altered by the branch channels. Although the overall direction of the branches may be assumed to be radial, there are portions of a branch channel which have ϕ and z components, due to zigzagging of the channel. The polarization in ϕ and z directions is created when the charge in the highly conducting tortuous branch leader channels is redistributed due to currents flowing along the channel. Let us model the non-radial part of the branches as short highly conducting thin wires of length l distributed with number density n in the non-conducting medium (see Figure 1a). When the external field E is applied parallel to l, the wire acquires a dipole moment due to charges $\pm q$ at its ends. To neutralize E in the middle of the wire, q must be such that $2q/[4\pi\varepsilon_0(l/2)^2] = E$, i.e., $q = (\pi/2)l^2\varepsilon_0 E$. The polarization $P = (K-1)\varepsilon_0 E = nql = (\pi/2)nl^3\varepsilon_0 E$, and the effective dielectric permittivity is $K = 1 + (\pi/2)nl^3$. The average distance between the wires $\sim n^{-1/3}$ is comparable to the length of the wire l, leading to $K - 1 \sim 1$. In this paper we focus on the effect of conductivity on the electromagnetic propagation characteristics, thus the numerical results are given for $\hat{K} = 1$.

2.2. Waveguide

[8] The waveguide serving as the model for the return stroke channel is composed of M cylindrical layers filled with media described by diagonal dielectric permittivity tensors (1), with boundaries ρ_k, $k = 1 \ldots M-1$ (also $\rho_0 = 0$, $\rho_M = \infty$), so that the medium in the range $\rho_{k-1} < \rho < \rho_k$ has permittivity tensor $\hat{\varepsilon}_k$. In this paper, we only consider a case of three layers ($M = 3$, see Figure 1b), with the boundaries $b \equiv \rho_1$, $a \equiv \rho_2$ having the same meaning as in [*Wang*, 2010]:

[9] 1. $\rho < b$: The highly conducting core channel, with isotropic dielectric permittivity.

[10] 2. $b < \rho < a$: The "metamaterial" corona with anisotropic diagonal effective dielectric permittivity.

[11] 3. $\rho > a$: Non-conducting air, with unit dielectric permittivity.

[12] This model is a generalized Goubau waveguide, which is defined as a highly conducting wire immersed in a dielectric medium [*Goubau*, 1950; *Baba and Rakov*, 2007].

2.3. Axially Symmetric TM Mode

[13] In general, the modes do not separate into TE and TM modes [*Jackson*, 1975, section 8.10]. However, they do if we assume the axial symmetry $\partial/\partial\phi \equiv 0$. Let us consider only the TM mode which has non-zero components H_ϕ, E_ρ, and E_z (TE modes cannot propagate at low frequencies due to a cutoff), and excitation of wave solutions $\propto e^{-i\omega t+ik_z z}$ with external source current densities j_z^e parallel to the axis. The solutions are

$$H_\phi = \Psi/Z_0 \tag{2}$$

$$E_z = \frac{i}{k_0\varepsilon_z\rho}\left(\frac{\partial(\rho\Psi)}{\partial\rho} - j_z^e\right) \tag{3}$$

$$E_\rho = \frac{k_z}{k_0\varepsilon_\rho}\Psi \tag{4}$$

where $Z_0 = \sqrt{\mu_0/\varepsilon_0}$ is the impedance of the free space and Ψ in uniform medium excited by uniform currents ($\partial\varepsilon/\partial\rho = 0$, $\partial j_z/\partial\rho = 0$) satisfies equation

$$\frac{\partial}{\partial\rho}\left[\frac{1}{\rho}\frac{\partial(\rho\Psi)}{\partial\rho}\right] + k_\rho^2\Psi = 0 \tag{5}$$

where

$$k_\rho = \sqrt{\varepsilon_z\left(k_0^2 - k_\rho^2/\varepsilon_\rho\right)} \tag{6}$$

chosen so that $\Im k_\rho > 0$. The most general solution of this equation is

$$\Psi(\rho) = AC_1^{(1)}(k_\rho\rho) + BC_1^{(2)}(k_\rho\rho)$$

where $C_\alpha^{(1,2)}$ are any of the independent Bessel functions J, Y, $H^{(1)}$ or $H^{(2)}$ of order α. In the last medium ($k = M$), the field is outward-propagating or evanescent at $\rho \to \infty$, giving

$$\Psi(\rho) = A_M H_1^{(1)}(k_{\rho,M}\rho)$$

In intermediate regions, it is convenient to choose

$$\Psi(\rho) = A_k H_1^{(1)}(k_{\rho,k}\rho) + B_k H_1^{(2)}(k_{\rho,k}\rho)$$

where the first term corresponds to an outward wave, while the second to an inward wave. In the first layer ($k = 1$) the boundary condition of finite fields at $\rho = 0$ dictate that $A_1 = B_1$, giving

$$\Psi(\rho) = 2A_1 J_1(k_{\rho 1}\rho)$$

The electric field E_z (3) is expressed in terms of C_0 using

$$\frac{1}{\rho}\frac{\partial[\rho C_1(k_\rho\rho)]}{\partial\rho} = k_\rho C_0(k_\rho\rho)$$

[14] The coefficients A_k, B_k are found by matching the fields H_ϕ and E_z at the boundaries between layers. For arbitrary number of layers, it is convenient to implement the recursive procedure used in the full-wave method [*Lehtinen and Inan*, 2008], which guarantees the absence of numerical instabilities. The stability of this method relies on the separation into outward and inward waves in each layer, which motivates the use of Hankel functions. The symmetric TM mode of the waveguide is found in the absence of sources by matching the impedances $Z_k = E_z(\rho_k)/H_\phi(\rho_k)$ at the layer boundaries. The numerical solution of this problem is given in section 3.2, and an approximate solution for a three-layer waveguide (Figure 1b) is given in Appendix A.

2.4. Time- and Space-Domain Formulation

[15] We specify as the boundary conditions the perfectly conducting planes at $z = 0$ and $z = L$, so that $E_\rho = 0$ on those planes. This restricts the values of k_z to $k_{z,n} = \pi n/L$, where $n = -\infty \ldots \infty$ is an integer. The external current at each frequency ω and axial wave number $k_{z,n}$ is obtained using Fourier (cosine) transform

$$j_z^e(\rho, k_{z,n}, \omega) = \frac{1}{L}\int_0^L j_z^e(\rho, z, \omega)\cos k_{z,n}z\,dz \tag{7}$$

Taking $j_z^e(\rho, k_{z,n}, \omega)$ as the source, we calculate the distribution of fields $H_\phi(\rho)$ and $E_z(\rho)$ in the generated wave $\propto e^{-i\omega t+\mathrm{k}_z z}$. From these, we can obtain other quantities such as E_ρ and the induced conductivity currents j_z. The space-domain solution at a fixed frequency is obtained by taking the inverse Fourier transform $k_z \to z$

$$H_\phi(\rho, z, \omega) = \sum_n H_\phi(\rho, k_{z,n})e^{jk_{z,n}z}$$

and analogously for other quantities. The time domain solutions are found by taking a Fourier transform $\omega \to t$.

[16] We choose the external current such that it flows only in the core of the channel (current density j_z^e is uniform at $\rho < b$) and the source is localized just above the ground at $z = +0$, i.e., $j_z^e(\rho, z, t) = \Omega(b-\rho)\iota(t)\delta(z-0)/(\pi b^2)$, where Ω is the step function, $\iota(t)$ is the time profile of the total current moment and the notation $\delta(z - 0)$ means that the delta function is included in the integration in equation (7). Because of the conductivity in the core, there is an induced current with density j_z, which partially cancels j_z^e. We find the source $\iota(t)$ by fixing the total core current $I_0(t) = I(z = 0, t) = \int_0^b (j_z + j_z^e)2\pi\rho d\rho$ flowing through $z = 0$. In order to do this, we have to rescale $j_z^e(\rho, z, \omega)$ at each frequency ω so that the core current calculated by the model matches the Fourier components of I_0, i.e., $I(z = 0, \omega)$.

3. Results

3.1. The Current Wavefront Propagation

[17] We performed the time domain calculations for the driving current waveform given by a double exponential

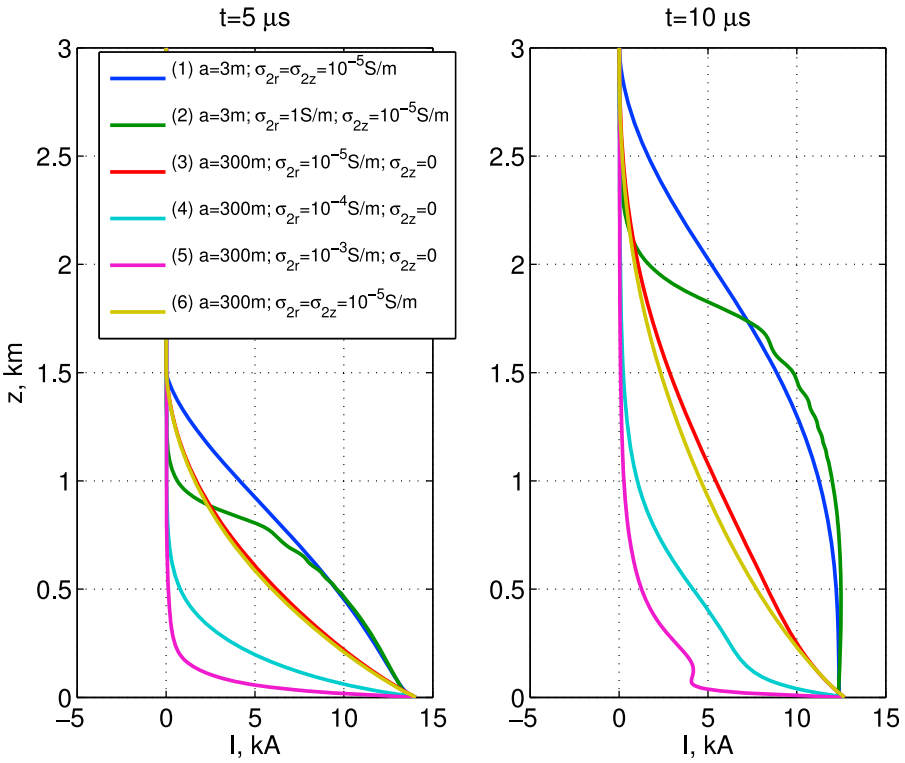

Figure 2. Current profiles in the channel driven by the Bruce-Golde model current at $z = 0$, at two selected moments of time, (left) $t = 5$ μs and (right) $t = 10$ μs, for all six different parameters of the corona.

[*Bruce and Golde*, 1941]: $I_0(t) = I_m(e^{-at} - e^{-bt})$ at $t > 0$, where $I_m = 20$ kA, $a = 4.4 \times 10^4$ s^{-1}, $b = 4.6 \times 10^5$ s^{-1} [*Volland*, 1995, p. 113], with the length of the channel of $L = 3$ km. We modeled six different waveguides. For all of these, the highly conducting core channel is the same, $b = 3$ cm and $\sigma_1 = 10^4$ S/m [*Baba and Rakov*, 2009, section 1.2], but coronas have different parameters:

[18] 1. "Standard" (in size and conductivity) isotropic corona with $a = 3$ m, $\sigma_{2\rho} = \sigma_{2z} = 10^{-5}$ S/m [*Maslowski and Rakov*, 2006];

[19] 2. Anisotropic corona, extremely conducting in radial direction, with $a = 3$ m, $\sigma_{2\rho} = 1$ S/m, $\sigma_{2z} = 10^{-5}$ S/m;

[20] 3. Large ($a = 300$ m) corona with a standard conductivity $\sigma_{2\rho} = 10^{-5}$ S/m but non-conducting in the axial direction ($\sigma_{2z} = 0$);

[21] 4. Same as Case (3), but with a higher radial conductivity $\sigma_{2\rho} = 10^{-4}$ S/m;

[22] 5. Same as Cases (3) and (4), but with an even higher radial conductivity $\sigma_{2\rho} = 10^{-3}$ S/m;

[23] 6. Large isotropic corona, i.e., same as Case (3) but with an equal axial conductivity $\sigma_{2z} = 10^{-5}$ S/m.

[24] The justification for this choices is discussed below in section 4.2.

[25] The results are presented in Figures 2–4. Figure 2 demonstrates the current distributions at two selected moments of time. We see that the wavefronts for all simulated waveguides are rather gradual. Case (2), which has the highest radial conductivity of the corona $\sigma_{2\rho} = 1$ S/m, also has the steepest wavefront, whose shape is actually determined by the driving current. From the solution of the dispersion equation presented in section 3.2, will see that this is related to the fact that attenuation of short wavelengths is smaller for Case (2) than for all other cases. We note that for more abrupt current onset (not presented here) this case produces an even steeper wavefront, with leading oscillations, similar to those obtained by [*Moini et al.*, 2000, Figure 3e]. Some leading oscillations are also noticeable for Case (5) which, similarly to Case (2), also has a relatively high radial conductivity of the corona $\sigma_{2\rho} = 10^{-3}$ S/m.

[26] There is an uncertainty in determining the wavefront speed since the wavefront gets dispersed as it propagates, as seen in Figure 2. One of the ways to define it is to track the propagation of a fixed current level. The wavefront speeds calculated at the level of $0.2I_{\max}$ are presented in Figure 3. The cutoff at ~10–20 μs is due to the wavefront reaching the upper boundary at $z = L = 3$ km. All models give lower speeds than the "standard" model of corona of Case (1); the coronas with larger radii and larger radial conductivities in general produce lower wavefront speeds. However, one should be careful in interpreting this result because some of the "slowdown" may be due to the stretching out of the wavefronts.

[27] The radial electric field E_ρ calculated at the distance of $\rho = 0.1$ m from the axis and at the altitude of $z = 20$ m is presented in Figure 4. The location was chosen to facilitate the comparisons with measurements of *Miki et al.* [2002]. The measured E_ρ, presented by *Miki et al.* [2002], is a negative pulse for a negative cloud-to-ground discharge, i.e., a positive return stroke current flowing up. The front and tail of this pulse, as explained by *Maslowski and Rakov*

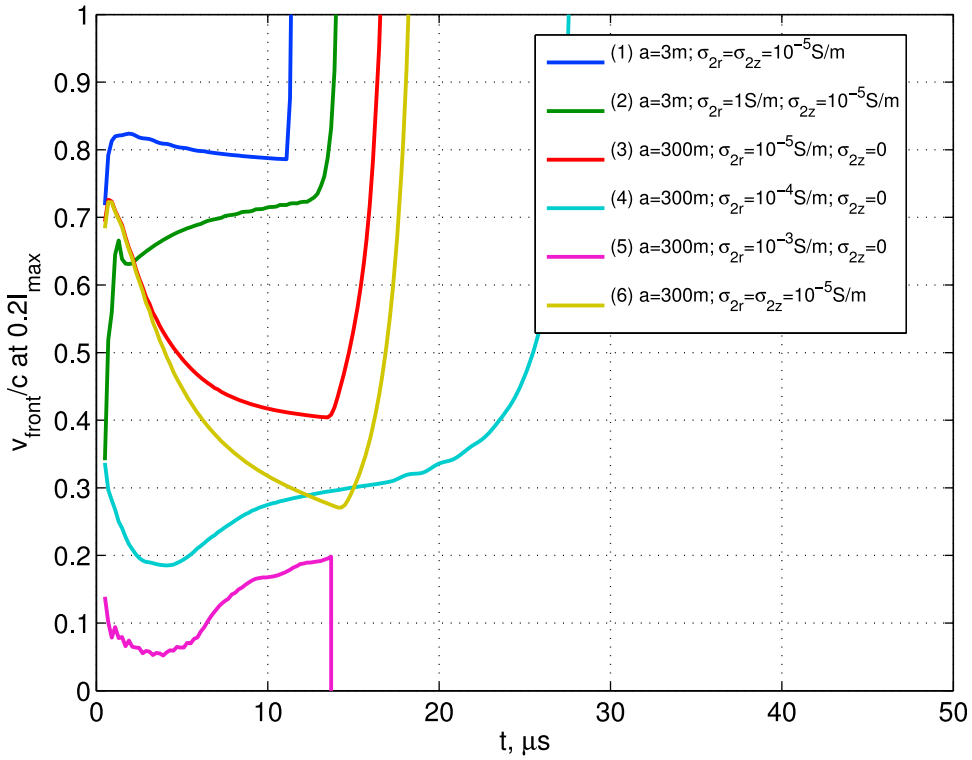

Figure 3. The speed of the wavefront measured at the level of $0.2I_{\max}$ for all six different parameters of the corona.

[2006, Figure 2a], are due to different processes. The front (negative change in E_ρ) is due to the leader, which was not simulated here. The tail (positive change) is due to the return stroke, and should be compared to the fronts of the pulses in Figure 4. Because of the negative charge in the channel deposited by the leader, which was not taken into account by the present simulation, there is a positive bias in the results of Figure 4, compared to the results of *Miki et al.*

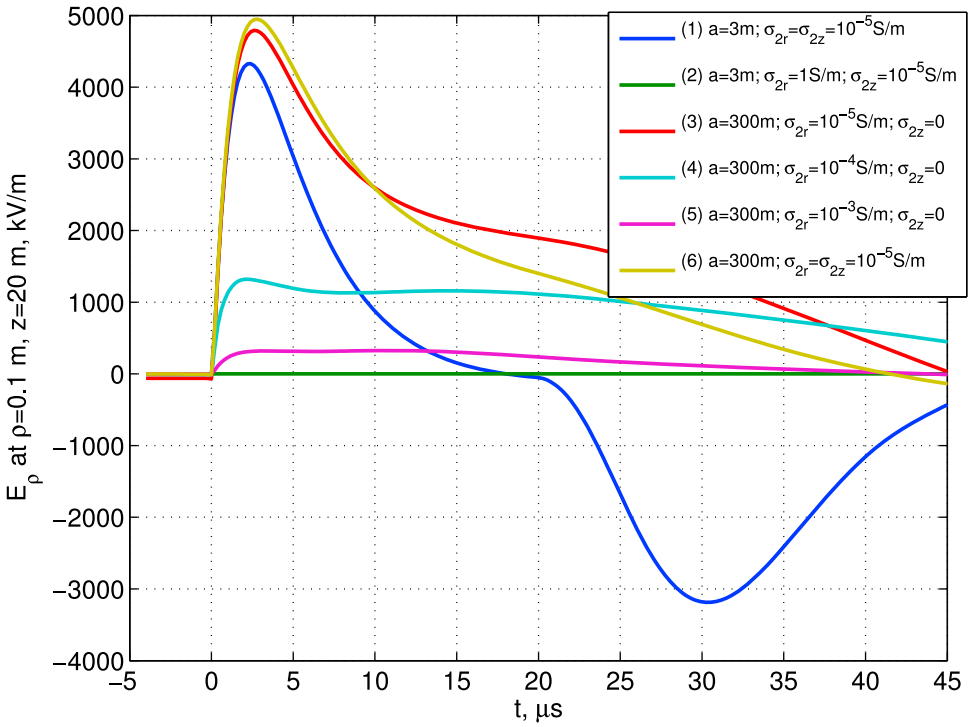

Figure 4. The radial electric field at $z = 20$ m and $\rho = 0.1$ m.

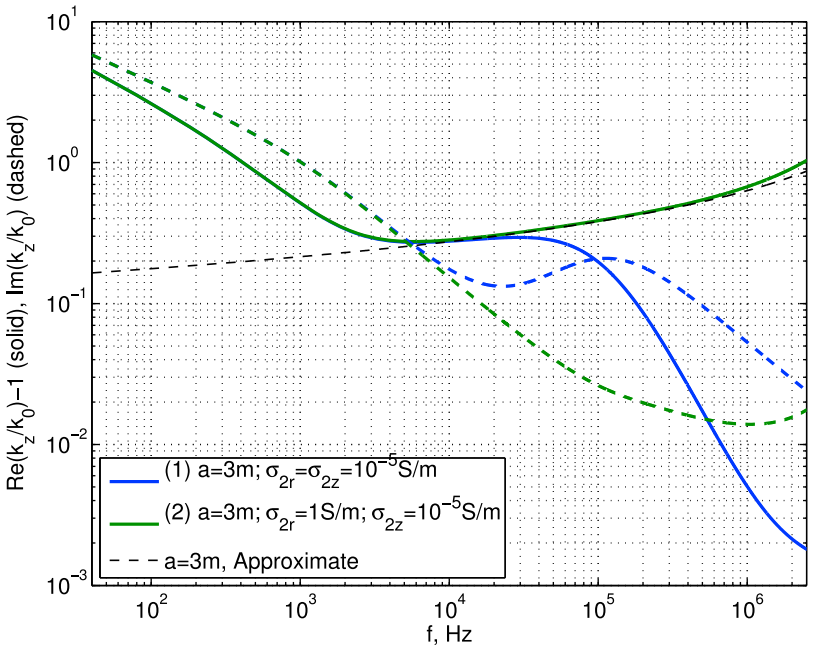

Figure 5. The normalized wave number k_z/k_0, for Cases (1) and (2) which have a = 3 m. Also shown is the approximate solution (A9).

[2002]. The field always gradually relaxes to zero, but because of this bias (which also relaxes to zero), the relaxation is different in the present simulation than in the measurements.

[28] Case (2) does not produce a large field (only ~80 V/m), due to high radial conductivity of corona. However, we should remember that the high radial conductivity is due to discrete structures (branches), so the calculation results present statistically averaged measurement. If the instrument is actually located between branches, the measured field will be higher. Cases (4) and (5) produce fields comparable to those measured by *Miki et al.* [2002], for the similar driving current. Note that the low-radial conductivity corona ($\sigma_{2\rho}$ = 10^{-5} S/m) produces E_ρ several times higher than the measured, the best fit being given by $\sigma_{2\rho} = 10^{-4}$ S/m of Case (4). In both Cases (4) and (5), the field relaxation to zero is rather slow, because the removal of charge is prevented by low axial conductivity of the corona (σ_{2z} = 0), with a timescale exceeding the radial relaxation timescale of $\varepsilon_0/\sigma_{2\rho} \lesssim 1$ μs. In the measurements, this relaxation is

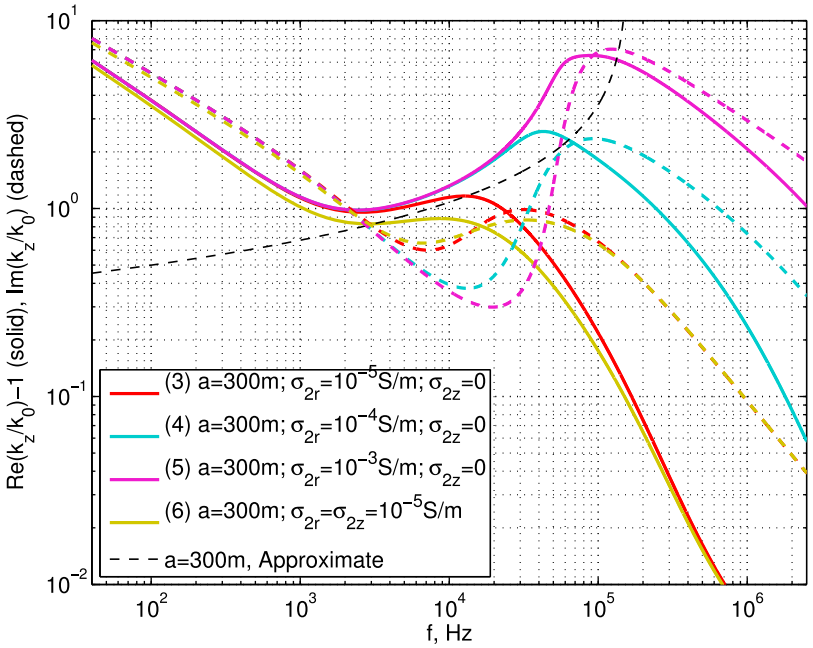

Figure 6. The normalized wave number k_z/k_0, for Cases (3)–(6) which have a = 300 m. Also shown is the approximate solution (A9).

canceled by the relaxation of the negative charge initially deposited by the leader, as discussed in the previous paragraph.

3.2. Numerical Solution of the Dispersion Equation

[29] The dispersion equation relates the axial wave number k_z of the axially symmetric TM mode (in the absence of sources) to the frequency of the wave ω. In this work, k_z was numerically found for each ω by matching the impedance E_z/H_ϕ at each layer boundary ρ_k, $k = 1 \ldots M - 1$. Figures 5 and 6 present the solutions of the dispersion equation for k_z for the frequency range from 40 Hz to 2.5 MHz for the Cases (1)–(6) considered above. Figures 5 and 6 correspond to two different corona radii $a = 3$ or 300 m. For different corona radii, the approximate formula (A9) gives different results which are plotted in Figures 5 and 6 with dashed thin black lines.

[30] Analyzing Figure 5, in which the results for a smaller corona radius ($a = 3$ m) are presented, we see that the approximate solution (A9) is rather accurate for Case (2) for frequencies above a few kHz. It even gives an accurate result for the "standard" corona (Case (1)) for a narrow interval around ~10 kHz. In general, we see that the approximate solution is more accurate when the spatial attenuation is low (i.e., $\Im(k_z/k_0)$ is small), but deviates from the numerical solution at frequencies which give higher spatial attenuation.

[31] The approximate solution (A9) for a large corona ($a =$ 300 m) is in general less accurate, as seen in Figure 6. The frequency range in which it is most accurate is widest (~1–100 kHz) for Case (5), for which also the spatial attenuation is the lowest in this range. This is related to the fact that this Case has the slowest wavefront speed, since in the same frequency range the phase velocity ($\sim k_0/k_z$, the inverse of the plotted value) is also the lowest.

4. Discussion

4.1. Relation to the Transmission Line (TL) Model

[32] The equations for the voltage V and current I in a transmission line are [*Harrington*, 2001, sections 2–6]

$$\frac{dV}{dz} = -IZ \tag{8}$$

$$\frac{dI}{dz} = -VY \tag{9}$$

with the following values per unit length: impedance $Z = R - i\omega L$, shunt admittance $Y = G - i\omega C$, resistance R, inductance L, shunt conductance G, and capacitance C. We have only highly conducting material and the TL is completely isolated, so we assume $R = 0$ and $G = 0$. The dispersion equation is

$$\frac{\omega^2}{k_z^2} = v_{ph}^2 = -\frac{\omega^2}{ZY} = \frac{1}{LC}$$

To find $C = \lambda/V$, where V is the potential charge per unit length λ, we note that the charge in our waveguide is accumulated on the outer boundary of the corona, at $\rho = a$. At zero frequency, the field at $\rho > a$ is $E_\rho = \lambda/(2\pi\varepsilon_0\rho)$, which gives $V = \lambda \log(\rho_0/a)/(2\pi\varepsilon_0)$, relative to distance ρ_0. In a regular transmission line, this is the distance to the second conductor. The biggest conductor present in the environment of the lightning is the conducting Earth. However, its effect is creation of an image lightning channel, which, with the assumption that the lightning channel is strictly vertical, lies on the same axis as the real channel, so that the axial symmetry is preserved. The effects of the Earth may be treated by boundary conditions at the point of the attachment of the channel to the Earth. Thus, here we assume that the second conductor is at infinity, but avoid the infinity in the final answer by noticing that at non-zero frequency, ρ_0 has to be chosen as a typical evanescence length in the radial direction. If the wave in the waveguide is slower than the speed of light, i.e., $k_z/k_0 = \beta > 1$, we have $k_\rho = ik_0\sqrt{\beta^2 - 1}$, i.e., the evanescence length is $\rho_0 \sim 1/k_0$ times a factor of the order unity, which is not important under the logarithm sign. Thus, we have

$$C \approx \frac{2\pi\varepsilon_0}{\log[1/(k_0 a)]}$$

The inductance is $L = \phi/I$, where ϕ is the magnetic field flux around the TL per unit length. Since all the current flows in the highly conducting core, at $\rho < b$, we have $B = \mu_0 I/(2\pi\rho)$ at $\rho > b$, integrating which out to distance ρ_0, we find $\phi = \mu_0 I \log(\rho_0/b)/(2\pi)$. Again taking $\rho_0 \sim 1/k_0$, we get

$$L \approx \frac{\mu_0}{2\pi}\log[1/(k_0 b)]$$

Substituting these into the dispersion equation, we find

$$v_{ph}^2 = c^2 \frac{\log[1/(k_0 a)]}{\log[1/(k_0 b)]}$$

the same answer as (A9) obtained in Appendix A.

4.2. The Measured Corona Conductivity and the "Metamaterial"

[33] In this paper, we generally assume that the high radial conductivity is due to leaders branching off the main leader channel of the lightning, unlike the usual assumption that the corona conductivity is due to streamers [e.g., *Cooray*, 1993], whose conductivity is only of the order of 0.1 S/m [*Raizer*, 1991, p. 434]; for example, in simulation Case (2) we assumed $\sigma_{2\rho} = 1$ S/m. Such a high conductivity is in apparent contradiction with measurements of *Miki et al.* [2002] and the analysis of their data by *Maslowski and Rakov* [2006], who concluded that the average conductivity of the corona at $\rho > 0.1$ m is only of the order of 10^{-6}–10^{-5} S/m. The radial field produced in simulation Case (2) is also too low and contradicts the measurements. However, the simulation gives the average field which may have been measured either inside or outside a branch leader channel. It may be possible that the leaders that give the corona its high radial conductivity were just "missed" by the electric field detector, because they are not very densely packed (low "filling factor").

[34] If the leader channel conductivity is 10^4 S/m, then the "filling factor" required for Case (2) is 10^{-4}, and only 10^{-8}

for Case (4) and 10^{-7} for Case (5). The Cases (4) and (5) could support even streamer conductivity with filling factors of 10^{-3} and 10^{-2}, respectively. However, the large size of the corona considered in this Case (a = 300 m) makes it unlikely that the streamers do not form into leaders at this scale.

4.3. The Size and Shape of the Leader Branch Corona

[35] Recent observations of natural lightning using an optical instrument with a large dynamic range [*Lebedev et al.*, 2007] demonstrated the presence of leader branches of 1–3 m length. These branches were significantly fainter than the main channel, however, the discrete structure corroborates their leader nature (as opposed to streamer), so the conductivity inside of them is probably much higher than that of the medium occupied by streamers. The direction of these branches was rather chaotic, outward from the channel with bending along the channel axis in both directions. The model of this paper makes a simplifying assumption that the branches are strictly outward orthogonally to the axis of the channel. If the bending of these branches were small (compared to their length), the effects could be included by increasing the effective dielectric permittivity of the corona K_z, as discussed in the end of section 2.1. A more exact treatment of sharply bent branches, however, would require a more sophisticated model.

[36] A corona with a radius of 300 m (Cases (3)–(6)), compared to these observations seems to be a rather extreme case. However, one may consider this to be the representation of the long branches, such as those at the top of the lightning channel in the work by *Lebedev et al.* [2007, Figures 5 and 6], distinct from the faint leader branches shown in Figure 8 of the same paper.

5. Conclusions

[37] We have presented a "metamaterial" corona model of the return stroke channel, which takes into account the effect of the contribution of the branch leaders of the corona of the return stroke channel into its electrodynamic properties, without detailed modeling of each branch. This method may be refined in the future by taking into account, i.e., the dependence of the branch leader characteristics (such as conductivity and branching) on the distance from the central core, and opens new possibilities in the development of electrodynamic models of the return stroke [*Baba and Rakov*, 2007].

[38] The increase in the capacitive loading [*Baba and Rakov*, 2007] per unit length C due to the corona leads to the decrease of the velocity of the wave. The branches of length a effectively create a corona of radius a, which decreases the phase velocity by a factor of $\sqrt{\log[1/(k_0 b)]/\log[1/(k_0 a)]}$. Note that the branches may be arbitrarily long, and not restricted by the value of 300 m considered in the simulations for this paper. This capacitive loading may explain the abrupt dropping of the return stroke speed after passing each major branch [*Baba and Rakov*, 2009, section 1.2]. The upcoming time-dependent fractal lightning (TDFL) model [*Liang et al.*, 2010] will provide quantitative verification of the claims made in this paper. On the other hand, the results of this paper may be used in TDFL to model the effective characteristics of the waveguide with multiple branches, similarly to the approach by *Podgorski* [1991] who included extra circuit elements in his model of the lightning channel.

Appendix A: Approximate Solution of the Dispersion Equation

[39] For three layers, with a highly conducting core and relatively weakly conducting corona, all surrounded by vacuum, one may attempt an approximate analytical solution of the dispersion equation. We remind the reader that we have:

[40] 1. $\rho < b$: The highly conducting isotropic core channel, with dielectric permittivity $\varepsilon_1 = 1 + iN_1$, $N_1 \gg 1$, i.e., an isotropic medium which has $\varepsilon_{\rho 1} = \varepsilon_{\phi 1} = \varepsilon_{z1} = \varepsilon_1$ in equation (1).

[41] 2. $b < \rho < a$: The corona, composed, as explained in section 2.1, of a "metamaterial" with anisotropic effective dielectric permittivity given by a tensor with components $\varepsilon_{\rho 2} = 1 + iN_2$, $\varepsilon_{\phi 2} = \varepsilon_{z2} = K$, where $K \gtrsim 1$, $N_2 \gg 1$.

[42] 3. $\rho > a$: Non-conducting air, dielectric permittivity $\varepsilon_3 = 1$.

[43] The surface impedance for TM waves is defined [*Roberts*, 1953] as $Z = E_z/H_\phi$. We will use its dimensionless form

$$\zeta = \frac{Z}{Z_0} = \frac{E_z}{Z_0 H_\phi} = \frac{i}{\varepsilon_z k_0 \rho \Psi} \frac{\partial(\rho\Psi)}{\partial\rho} \tag{A1}$$

where $k_0 = \omega/c$ and $Z_0 = \sqrt{\mu_0/\varepsilon_0}$. For $\Psi = A\mathcal{C}_1^{(1)}(k_\rho\rho) + B\mathcal{C}_1^{(2)}(k_\rho\rho)$ (where $\Im k_\rho \geq 0$ and $\mathcal{C}$ are any of the Bessel functions J, Y, $H^{(1,2)}$),

$$\zeta = \frac{ik_\rho}{\varepsilon_z k_0} \frac{A\mathcal{C}_0^{(1)}(k_\rho\rho) + B\mathcal{C}_0^{(2)}(k_\rho\rho)}{A\mathcal{C}_1^{(1)}(k_\rho\rho) + B\mathcal{C}_1^{(2)}(k_\rho\rho)}$$

It is convenient to introduce normalized wave numbers $\beta = k_z/k_0$ and $\kappa = k_\rho/k_0$. For computational purposes and unlike section 2.3, where Hankel functions were used, here it is convenient to choose in the first and second layer $\mathcal{C}^{(1)} = J$ and $\mathcal{C}^{(2)} = Y$.

[44] The impedance ζ has to match at the boundaries between cylindrical layers because both E_z and H_ϕ are continuous. By the way, the sign of Re ζ determines the direction of energy flow, e.g., Re $\zeta < 0$ means that the energy is going from $\rho = 0$ outwards to $\rho = \infty$. We have the following impedance matching conditions:

[45] 1. At $\rho = b$ (boundary between the core channel and the corona):

$$\zeta_b = \frac{i\kappa_1 J_0(\kappa_1 k_0 b)}{(1 + iN_1) J_1(\kappa_1 k_0 b)} = \frac{i\kappa_2}{K} \frac{A_2 J_0(\kappa_2 k_0 b) + B_2 Y_0(\kappa_2 k_0 b)}{A_2 J_1(\kappa_2 k_0 b) + B_2 Y_1(\kappa_2 k_0 b)} \tag{A2}$$

[46] 2. At $\rho = a$ (boundary between the corona and the air):

$$\zeta_a = \frac{i\kappa_2}{K} \frac{A_2 J_0(\kappa_2 k_0 a) + B_2 Y_0(\kappa_2 k_0 a)}{A_2 J_1(\kappa_2 k_0 a) + B_2 Y_1(\kappa_2 k_0 a)} = \frac{i\kappa_3 H_0^{(1)}(\kappa_3 k_0 a)}{H_1^{(1)}(\kappa_3 k_0 a)} \tag{A3}$$

[47] In these expressions, we must use, according to equation (6):

$$\kappa_1 = \sqrt{1 + iN_1 - \beta^2} \tag{A4}$$

$$\kappa_2 = \sqrt{K - \beta^2 K/(1 + iN_2)} \tag{A5}$$

$$\kappa_3 = \sqrt{1 - \beta^2} \tag{A6}$$

Assume (i) return stroke speed of the order of speed of light, $\beta \sim 1$; (ii) high conductivity, $N_{1,2} \gg 1$; (iii) moderate effective dielectric permittivity of corona in ϕ and z directions, $K \gtrsim 1$ but $K \ll N_{1,2}$; and (iv) thin channel compared to the vacuum wavelength, $k_0 a \ll 1 \Rightarrow k_0 b \ll 1$.

[48] Using assumptions (i)–(iii) in (A4)–(A6), we get

$$\kappa_1 \approx \sqrt{iN_1} = (1 + i)\sqrt{N_1/2}, \qquad \kappa_2 \approx \sqrt{K}$$

For a highly conducting core channel, we may outright assume that $E_z(\rho = b) = 0$, i.e., $\zeta_b = 0$. However, to find corrections due to finite conductivity, let us use the approximate κ_1 in the first equality of equation (A2). We have a dimensionless parameter $b/\delta = \sqrt{f/f_0}$, where $\delta = \sqrt{2/N_1}/k_0$ is the skin depth, and $f_0 = R/\mu_0$, where $R = 1/(\pi b^2 \sigma)$ is the resistance per unit length. The argument of the Bessel function is $\kappa_1 k_0 b = (1 + i)b/\delta$. Assuming $b = 3$ cm, $\sigma = 10^4$ S/m [*Baba and Rakov*, 2009, section 1.2], we find $R = 0.035$ Ω/m and $f_0 \approx 30$ kHz. Consider two cases:

[49] 1. $f \gg f_0 \Rightarrow b \gg \delta \Rightarrow |\kappa_1 k_0 b| \gg 1$. Using asymptotic formulas for large argument, we have $J_0/J_1 \approx -i$ and

$$\zeta_b \approx \frac{1}{\sqrt{iN_1}} = \frac{1 - i}{\sqrt{2N_1}}; \quad |\zeta_b| \ll 1 \tag{A7}$$

[50] 2. $f \ll f_0 \Rightarrow b \ll \delta \Rightarrow |\kappa_1 k_0 b| \ll 1$. Using asymptotic approximation $J_0 \approx 1$, $J_1 \approx \kappa_1 k_0 b/2$, we have

$$\zeta_b \approx \frac{2}{k_0 b N_1} = \frac{2\pi f_0 b}{c} \tag{A8}$$

Using the above value for f_0, we get $\zeta_b \approx 2 \times 10^{-5} \ll 1$.

[51] Setting $\zeta_b = 0$ in the second equality of (A2), we immediately find (up to an unimportant factor)

$$A_2 = Y_0(\kappa_2 k_0 b), \qquad B_2 = -J_0(\kappa_2 k_0 b)$$

Substitute these into equation (A3), and use $\kappa_2 k_0 b \ll 1$ and $\kappa_{2,3} k_0 a \ll 1$, which follow from assumption (iv). We use the asymptotic forms of J, Y and $H^{(1)} = J + iY$ for small argument. Equation (A3) becomes

$$\zeta_a = -ik_0 a \log\left(\frac{a}{b}\right) = i\kappa_3^2 k_0 a \left[\log\left(\frac{1}{k_0 a}\right) + u\right]$$

where $u = i\pi/2 + \log 2 - \gamma - \log \kappa_3$, $\gamma \approx 0.5772$ is the Euler-Mascheroni constant, $\kappa_3 = \sqrt{1 - \beta^2}$, Im $\kappa_3 > 0$. From here, neglecting u compared to $\log[1/(k_0 a)] = |\log(k_0 a)|$, $\log[1/(k_0 b)]$, we have an approximate solution

$$(\beta)^2_{\text{approx}} = \frac{\log[1/(k_0 b)]}{\log[1/(k_0 a)]} \tag{A9}$$

Appendix B: Isotropic Corona

[52] The return stroke channel model making use of a wire immersed in an artificial medium with high isotropic ε_2 has been introduced by *Moini et al.* [2000]. The value of ε_2 used by workers in this class of models [*Baba and Rakov*, 2007], however, is usually chosen artificially in order to fit the observed return-stroke speed, and its physical nature is not given. Let us analyze our dispersion relation to see the origins of the speed reduction. The only place we used the anisotropy of the corona is in the relation $\kappa_2 = \sqrt{K - \beta^2 K/(1 + iN_2)} \approx \sqrt{K}$, in which the dependence on β disappears due to the high value of N_2. This can also occur in isotropic medium, $\kappa_2 = \sqrt{\varepsilon_2 - \beta^2} \approx \sqrt{\varepsilon_2}$ when ε_2 has a high absolute value, i.e., $\beta^2 \ll \sqrt{|\varepsilon_2|}$.

[53] The high absolute value of ε_2 may occur, e.g., when there is a large contribution from conductivity. However, the conductivity cannot be too high, otherwise the corona will be just a part of the high-conductivity channel and we will regress to the single-wire model, which does not give the speed reduction [*Volland*, 1981]. Neither can it be too low, in which case the resistive losses will become too high. A result very similar to "metamaterial" corona model may be achieved by taking a large real permittivity K_2. However, this situation may not have a valid physical basis. It may be possible that there may be a mechanism similar to that described in section 2.1, when the polarization is produced by the currents in the isolated streamer and leader pieces.

[54] **Acknowledgments.** This work was supported by DARPA grant HR0011-10-1-0058 and NSF grant ATM-0836326.

References

Baba, Y., and V. A. Rakov (2005), On the mechanism of attenuation of current waves propagating along a vertical perfectly conducting wire above ground: Application to lightning, *IEEE Trans. Electromagn. Compat.*, *47*(3), 521–532, doi:10.1109/TEMC.2005.850690.

Baba, Y., and V. A. Rakov (2007), Electromagnetic models of the lightning return stroke, *J. Geophys. Res.*, *112*, D04102, doi:10.1029/2006JD007222.

Baba, Y., and V. A. Rakov (2009), Present understanding of the lightning return stroke, in *Lightning: Principles, Instruments and Applications*, edited by H. D. Betz, U. Schumann, and P. Laroche, chap. 1, Springer, Dordrecht, Netherlands.

Bruce, C. E. R., and R. H. Golde (1941), The lightning discharge, *J. Inst. Electr. Eng., Part 2*, *88*, 487–505, doi:10.1049/ji-2.1941.0065.

Carlson, B. E., C. Liang, N. G. Lehtinen, M. B. Cohen, D. S. Lauben, and U. S. Inan (2011), Examining lightning channel electrical properties with time domain fractal lightning modeling, paper presented at XXX URSI General Assembly and Scientific Symposium of International Union of Radio Science, Int. Union of Radio Sci., Istanbul, Turkey.

Cooray, V. (1993), A model for subsequent return strokes, *J. Electrostatics*, *30*, 343–354, doi:10.1016/0304-3886(93)90088-O.

Goubau, G. (1950), Surface waves and their application to transmission lines, *J. Appl. Phys.*, *21*, 1119–1128, doi:10.1063/1.1699553.

Harrington, R. F. (2001), *Time-Harmonic Electromagnetic Fields*, IEEE Press, New York.

Jackson, J. D. (1975), *Classical Electrodynamics*, 2nd ed., John Wiley, New York.

Lebedev, V. B., G. G. Feldman, B. N. Gorin, Y. V. Shcherbakov, V. S. Syssoev, V. A. Rakov, M. A. Uman, and R. C. Olsen (2007), Test of the image converter cameras complex for research of discharges in long air gaps and lightning, paper presented at the 13th International Conference on Atmospheric Electricity, Int. Comm. on Atmos. Electr., Beijing.

Lehtinen, N. G., and U. S. Inan (2008), Radiation of ELF/VLF waves by harmonically varying currents into a stratified ionosphere with application to radiation by a modulated electrojet, *J. Geophys. Res.*, *113*, A06301, doi:10.1029/2007JA012911.

Liang, C., B. E. Carlson, N. G. Lehtinen, M. B. Cohen, D. S. Lauben, and U. S. Inan (2010), Toward a time-domain fractal lightning simulation,

Abstract AE23A-01 presented at 2010 Fall Meeting, AGU, San Francisco, Calif., 13–17 Dec.

Maslowski, G., and V. A. Rakov (2006), A study of the lightning channel corona sheath, *J. Geophys. Res.*, *111*, D14110, doi:10.1029/2005JD006858.

Miki, M., V. A. Rakov, K. J. Rambo, G. H. Schnetzer, and M. A. Uman (2002), Electric fields near triggered lightning channels measured with pockels sensors, *J. Geophys. Res.*, *107*(D16), 4277, doi:10.1029/2001JD001087.

Moini, R., B. Kordi, G. Z. Rafi, and V. A. Rakov (2000), A new lightning return stroke model based on antenna theory, *J. Geophys. Res.*, *105*, 29,693–29,702, doi:10.1029/2000JD900541.

Podgorski, A. S. (1991), Three-dimensional time domain model of lightning including corona effects, paper presented at 1991 International Aerospace and Ground Conference on Lightning and Static Electricity, NASA, Cocoa Beach, Fla.

Raizer, Y. P. (1991), *Gas Discharge Physics*, Springer, New York.

Rakov, V. A. (1998), Some inferences on the propagation mechanisms of dart leaders and return strokes, *J. Geophys. Res.*, *103*, 1879–1887, doi:10.1029/97JD03116.

Rakov, V. A. (2007), Lighting return stroke speed, *J. Lightning Res.*, *1*, 80–89.

Rakov, V. A., and F. Rachidi (2009), Overview of recent progress in lightning research and lightning protection, *IEEE Trans. Electromag. Compat.*, *51*(3), 428–442, doi:10.1109/TEMC.2009.2019267.

Roberts, T. E. (1953), Theory of the single-wire transmission line, *J. Appl. Phys.*, *24*(1), 57–67, doi:10.1063/1.1721134.

Volland, H. (1981), A wave guide model of lightning currents, *J. Atmos. Terr. Phys.*, *43*(3), 191–204, doi:10.1016/0021-9169(81)90038-6.

Volland, H. (Ed.) (1995), *Handbook of Atmospheric Electrodynamics*, vol. 1, CRC Press, New York.

Wang, N. (2010), The TEM wave characteristic impedance of lightning return stroke by multi-fractal theory, in *2010 Asia-Pacific International Symposium on Electromagnetic Compatibility*, pp. 1518–1521, Tsinghua Univ., Beijing, doi:10.1109/APEMC.2010.5475765.

N. G. Lehtinen, Department of Electrical Engineering, Stanford University, 350 Serra Mall, Stanford, CA 94305, USA. (nleht@stanford.edu)